Journal of Thermal Analysis and Calorimetry, Vol. 66 (2001) 659–673

POLYMORPHIC STUDY OF 2-(2-BENZOFURYL) Δ-2 IMIDAZOLINE

B. Legendre[1*], *G. Baziard-Mouysset*[2], *M. Anastassiadou*[2], *J. M. Leger*[3] *and M. Payard*[2]

[1]Laboratoire de Chimie Physique Minérale et Bioinorganique, EA401, Faculté de Pharmacie, rue J.B.Clément, 92290 Chatenây-Malabry, France
[2]Laboratoire de Chimie Pharmaceutique, EA819, Faculté de Pharmacie, 35 chemin des Maraîchers, 31400 Toulouse, France
[3]Laboratoire de Chimie Analytique, Faculté de Pharmacie, Université de Bordeaux III, 1 place de la Victoire, 33076 Bordeaux Cedex, France

(Received October 5, 2000; in revised form May 15, 2001)

Abstract

The compound 2-(2-benzofuryl) Δ-2 imidazoline, has been studied by DSC, TG, X-ray diffraction and thermomicroscopy.

We shall see that in the case of a study by DSC this compound presents a strange behaviour, which apparently is in contradiction with the thermodynamic rules. In a case of monotropy, if we have the α-phase (stable) and the γ-phase (metastable), after melting and cooling only the α-phase could crystallise. But this compound can give, according to the rate of cooling, the γ-phase metastable. The rate of cooling is of fundamental importance and the monotropic behaviour of this compound will be explained using the Gibbs function $G=f(T)$ for P=1 atm.

Keywords: crystal structure, imidazoline, metastable phase, polymorphism, thermal analysis

Introduction

2-(2-benzofuryl) Δ-2 imidazoline (Fig. 1) was synthesised, using the method described [1]. The chemical structure of this molecule collected by recrystallisation from cyclohexane is shown in Fig 1. This compound is of interest for pharmaceutical applications, described as an anti-depressant and vasodilator agent (antihypertensive drug) [1, 2]. Characterization of polymorphic forms constitutes an important aspect of drug development. Different polymorphs of a drug may exhibit significantly different biological activities due to their different solubility and dissolution rate [3].

* Author for correspondence. E-mail: bernard.legendre@cep.u-psud.fr

1418–2874/2001/ $ 5.00

Akadémiai Kiadó, Budapest
Kluwer Academic Publishers, Dordrecht

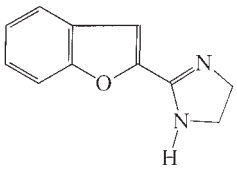

Fig. 1 Chemical structure of the molecule

The rate and duration of dissolution depends on the enthalpy of dissolution, which is in fact the sum of three terms and it can be expressed by the Eq. (1) deduced from the first law of thermodynamics:

$$\Delta_{\text{diss}} H = \int_{T_0}^{T_{\text{fus}}} (C_{\text{p}}^{\text{s}} - C_{\text{p}}^{\text{l}}) \text{d}T + \Delta_{\text{fus}} H + \Delta_{\text{mix}} H \quad (1)$$

The first term of the second part of this equation is generally slightly negative and is close to zero. The second term is the heat of fusion, this is always positive and differs for each crystallographic form. The third term $\Delta_{\text{mix}}H$ is the enthalpy of mixing of the solvent and of the compound in an undercooled liquid state, which may be positive or negative, but depends only on the liquid state. Since the main term for the modification of the enthalpy of dissolution is the enthalpy of fusion, we can easily infer therefore that bio-availability depends essentially on the heat of fusion and that the study of the polymorphism is of very great importance for the pharmacokinetics.

The aim of this work is to determine if polymorph transitions occur for this compound, and under which conditions the solid crystalline phase becomes stable from a thermodynamic point of view. The thermochemical behaviour was studied using: differential scanning calorimetry (DSC), thermogravimetric analyser (TG), thermomicroscopic analyser, powder and single-crystal X-ray diffraction.

Experiments and apparatus

Differential scanning calorimetry

A DSC 7 from Perkin Elmer was used. The apparatus was calibrated for temperature with the reference melting temperature were taken from literature [4] (indium 5N (NIST – National Institute of Standard and Technology): 156.634°C and tin 5N (Koch-Light) 231.9681°C), and calibration was performed for each heating rate. The heat of fusion of Indium is 28.44 J g^{-1} and the heat of fusion of tin is 59.22 J g^{-1}, respectively as recommended by the American Society for Materials ASM [5].

Pans were in aluminium based alloys and covers with holes were always used in order to keep the pressure constant. All the experiments were performed under dry nitrogen gas, with a flow of $2 \cdot 10^{-2}$ L min^{-1}.

Thermomicroscopic equipment composed of a heating stage from Mettler (FP5 and FP52) and an Olympus BH-2 microscope was used for interpreting the results obtained by DSC.

Thermogravimetric analyser

A thermobalance TGA 7 from Perkin Elmer was used. The calibration was made at different temperatures using Curie magnetic transition temperatures for the recommended alloys i.e. alumel (163°C), nickel (354°C), these temperature are given by Perkin Elmer. Calibration for mass was performed using a standard mass of 100 mg. All the experiments were performed under dry nitrogen, with a flow of $6 \cdot 10^{-2}$ L min^{-1}.

X-ray crystallographic analyse on powder

When using powder, analyse were performed using a Philips 1050 diffractometer and a 1729 Philips X-ray generator; a computer, controlling measurements and analyse, completed this equipment. The programs 'Gonio' and 'Rayon' are from Fraisse [6]. The anode used was made of CuK_α (λ=1.54051 Å).

For single crystal analyse, an Enraf-Nonius CAD-4 diffractometer equipped also with a CuK_α anode and a monochromator, selecting only CuK_{α_1} (λ=1.54178 Å) was used. Measurements were performed at room temperature.

Thermodynamic behaviour

In order to give a full description of this compound, the melting point was measured using a DSC method. The compound was submitted for DSC analyse with heating and cooling rates of 20°C min^{-1}.

The melting temperature and the heat of fusion were:

$$T_{fus}=148.5\pm0.5\ °C$$
$$\Delta_{fus}H=153.2\pm1\ J\ g^{-1}$$

This fusion was confirmed by thermomicroscopic observation. But if the same sample was heated again with the same rate, the observed values for the fusion were:

$$T_{fus}=138.3\pm0.5°C$$
$$\Delta_{fus}H=136.6\pm1\ J\ g^{-1}$$

A third cycle of heating and cooling gave a melting point close to 138°C, although heating 48 h later the DSC curve shows a small exothermic peak at about 100°C, and an endothermic peak at 148°C. For a cycle (heating and cooling) after the fusion, if a cooling rate of 1°C min^{-1} is used, on the next heating curve, the measured temperature of fusion is of 148°C.

From the above observation, two hypotheses can be advanced: there is either a solvate or a polymorphic case.

The thermogravimetric analyse did not show mass losses between 20 and 110°C and the percentage of mass loss was 0.95% between 130 and 160°C.

We must conclude that the observed phenomenon result not from a solvate but from polymorphism.

When two crystallographic phases exist at a fixed pressure of 1 atm and room temperature, only one is thermodynamically stable. The other one is metastable and there are two possibilities of unary type diagrams *P–T*, corresponding to either an enantiotropic or a monotropic behaviour.

Full determination of a unary phase diagram requires thermobarometric equipment performing DTA or DSC at different pressures. Without this kind of equipment we must be careful in order to interpret the results of DSC.

In the case of an enantiotropic behaviour, a first peak corresponding to the transition of the low temperature phase (α) to the high temperature phase (β) must be observed by DSC at a low heating rate (of course in a relative way) followed by a peak of higher energy for the melting temperature of the high temperature phase. However, if a fast heating rate is used, the α→β transition does not occur. In this case metastable fusion of the α-phase occurs and the heat of fusion is higher than the heat of fusion of the β-phase.

Since no peak of transition was observed, the heat of fusion at 148°C was always higher than the heat of fusion at 138°C, thus we could deduce therefore that polymorphic transition was not a case of enantiotropy.

Then the only other possibility was monotropic behaviour, and this had to be proved, and to be explained.

The phase at a melting point of 148°C will be called α and the phase at melting point of 138°C will be called γ (α and β are used in an enantiotropic case, α and γ in a monotropic case).

A DSC measurement with a heating rate of 1°C min^{-1} was performed on several samples to determine the purity of the crystallographic phase using the Perkin Elmer program, based on the Van't Hoff law (Fig. 2).

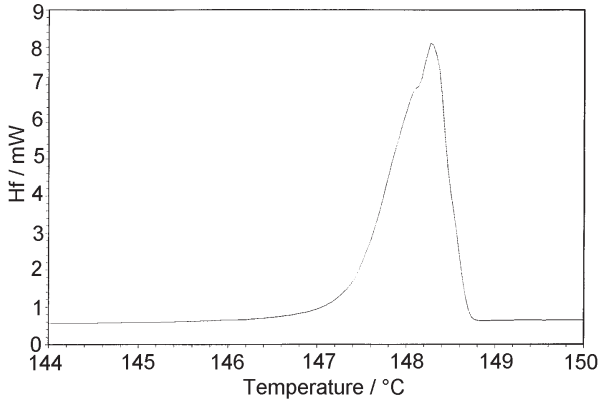

Fig. 2 DSC curve of melting V_c=1°C min^{-1}

The curve $T_{fus}=f(1/F)$ is presented in Fig. 3. A high coefficient of correction is necessary (6.46%). This may be explained by the shape of a small shoulder of the peak of fusion just before the maximum; this phenomenon was perfectly reproduced.

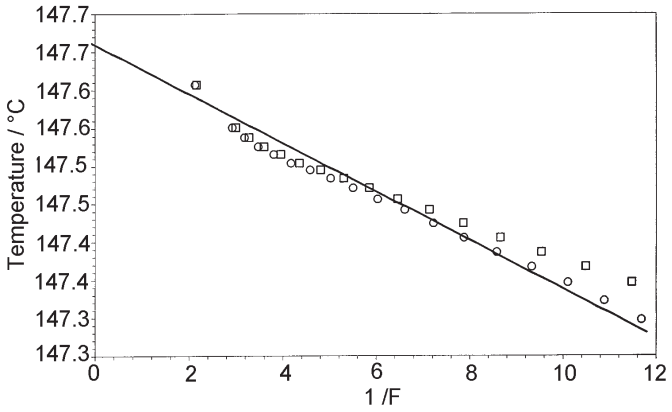

Fig. 3 Temperature of melting *vs.* of 1/*F* (melted fraction)

Closer examination of the crystallographic structure shows that two rings are tightly bound by a C_2–C'_2 bond and it is possible that at the melting temperature, when the intermolecular bonds are broken there is a possible rotation of one ring. Figures 4a and 4b; this explanation must be considered only as a hypothesis.

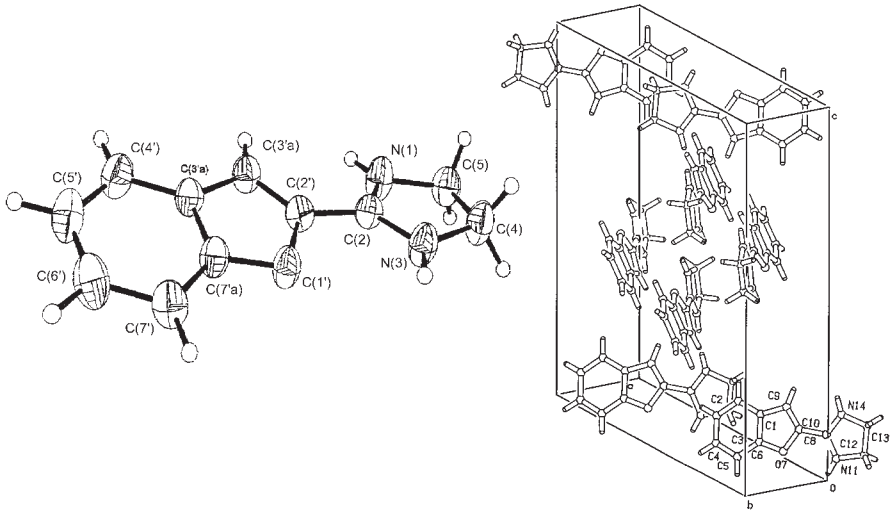

Fig. 4 Crystallographic structure (left); detail of one entity (right)

After the first measurement of the melting point temperature with a heating rate of 1°C min^{-1}, the cooling rate used with Perkin Elmer program is 200°C min^{-1}, a second cycle was performed with a heating rate of 1°C min^{-1} and a cooling rate of 1°C min^{-1} followed by a third heating with a heating rate of 1°C min^{-1}. In this case we

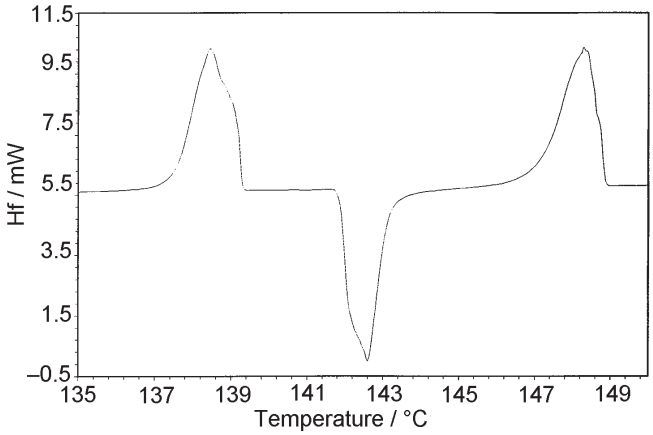

Fig. 5 DSC curve after cooling rate of 200°C min^{-1} (heating rate: V_c=1°C min^{-1})

observed two endothermic peaks and between them an exothermic peak (Fig. 5) with the following values for second and third cycles:

T_{fus}=137.52°C	T_{sol}=141.85°C	T_{fus}=147.12°C
$\Delta_{fus}H$=139.34 J g^{-1}	$\Delta_{sol}H$=–128.84 J g^{-1}	$\Delta_{fus}H$=134.47 J g^{-1}

The measured heat of fusion was lower than that of the first measurement. This is due to the vaporisation of a part of the sample, as it has been shown by TG measurements.

These results are explained by the fact, that after cooling, the γ-phase crystallises, then this phase melts at 138°C. The liquid is thermodynamically less stable than the α-phase and as heating is performed at a low rate, the α-phase has enough time to crystallise before melting at 148°C under stable thermodynamic conditions.

But apparently, this is in contradiction with the thermodynamic law of the phase rule. In the case of monotropy, if we have the α-phase (stable) or the γ-phase (metastable), after melting and cooling, only the α-phase should crystallise.

But as we have seen, using a lower heating rate of 1°C min^{-1} instead of 5 or 20°C min^{-1} the thermodynamic behaviour of the product is different.

As we may observe the equilibrium is reached only if we use low cooling rate (β≤1°C min^{-1}).

A series of experiments has been performed with various cooling rates from 80°C min^{-1} to 0.5°C min^{-1}, and a heating rate of 20°C min^{-1}.

The temperatures of solidification (T_s) *vs.* the cooling rate (β) are reported in Table 1. As we observe when the cooling rate increases the temperature of solidification decreases.

Table 1 Temperature of solidification (T_s) *vs.* cooling rate (β)

β/°C min^{-1}	–80	–40	–20	–10	–5	–2	–0.5
T_s/K	339	359	367	371	374	375	375
T_s/°C	+66	+86	+94	+98	+101	+102	+102

There is a linear relation between the temperature of the solidification and the cooling rate: T_s=376.14 – 0.45787 β; T is in (K) and β in (K min^{-1}).

Unfortunately, we could not use the values of the enthalpies of solidification for a calculation of $\Delta H=f(T)$ due to the fact that there is a small vaporisation. It is important to notice that for a cooling rate of – 40°C min^{-1} two peaks of crystallisation were observed and after, with a heating rate of 20°C min^{-1} two peaks of fusion were observed as shown in Figs 6a and 6b. For cooling rates lower than – 40°C min^{-1}, only one peak of solidification is observed and the crystallised phase is the α phase, the melting point of which is around 148°C, for faster cooling rates than – 40°C, only the metastable γ phase crystallises.

These temperatures of solidification will be used for an estimation of the difference between the Gibbs free energy curves of the liquid and of the solid (stable and metastable)

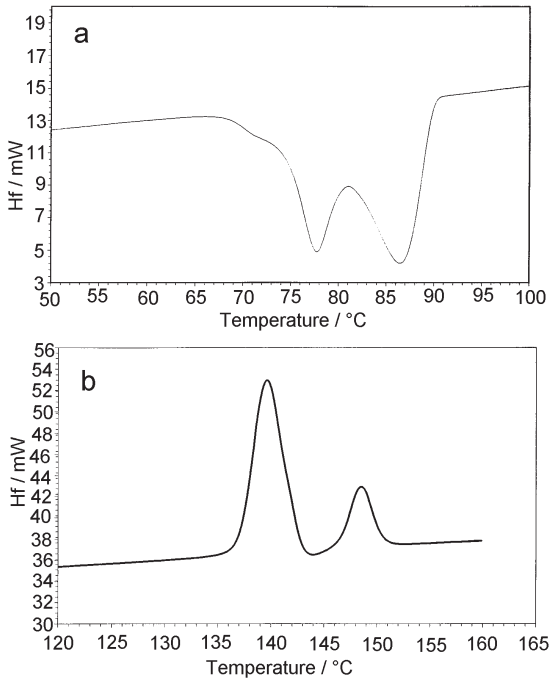

Fig. 6 DSC curve of a crystallisation of two forms β = – 40°C min^{-1} (a); DSC curve of melting after a cooling rate of 40 K min^{-1} (b)

$$\Delta G^{(l-s)} = \Delta_{fus} H (1 - T/T_{fus}) \quad (2)$$

Though this formula must be considered as an approximation, it is acceptable for a schematic representation.

Crystallographic data

Structure

The crystallographic structure was solved for a crystal having a melting point of about 148°C.

Table 2 Crystal data and structure refinement for 1

Identification code	p07	
Empirical formula	$C_{11}H_{10}N_2O$	
Formula mass	186.21 g mol^{-1}	
Temperature	296(2) K	
Wavelength	1.54178 Å	
Crystal system	Monoclinic	
Space group	C 2/c	
Unit cell dimensions	a = 18.671(2) Å	α = 90 deg
	b = 4.894(1) Å	β = 90.62(1) deg
	c = 20.009(2) Å	γ = 90 deg
Volume	1828.2(5) Å^3	
Z	8	
Density (calculated)	1353 kg m^{-3}	
Absorption coefficient	0.720 mm^{-1}	
F(000)	784	
Crystal size	0.25×0.20×0.15 mm	
Theta range for data collection	4.42 to 64.87 deg	
Index ranges	0≤h≤21, 0≤k≤5, –23≤1≤23	
Reflections collected	1507	
Independent reflections	1507 [R(int) = 0.0000]	
Refinement method	Full-matrix least-squares on F^2	
Data/restraints/parameters	1507/0/128	
Goodness-of-fit on F^2	1.066	
Final R indices [I>2σ(I)]	R1 = 0.0395, wR2 = 0.0935	
R indices (all data)	R1 = 0.0598, wR2 = 0.1061	
Extinction coefficient	0.0025(2)	
Largest diff. peak and hole	0.146 and –0.149 eA^{-3}	

The structure was solved by direct methods and refined using the SHELXS suite of programs (Sheldrick, 1993). Final residuals were R=0.039. Crystal data and structure refinement are listed in Table 2, the structure is presented in Fig. 4a. Fractional co-ordinates and equivalent thermal factors are given in Table 3. A diagram of the molecule with the atom numbering is shown in Fig. 4b. The 1,3-nitrogen substitutes show disorder of H, the position 1 being occupied by 0.5H and the position 3 by 0.5H.

The characteristics are presented in Tables 2 to 6.

Table 3 Atomic co-ordinates ($\cdot 10^4$) and equivalent isotropic displacement parameters ($Å^2 \cdot 10^3$) for 1. U(eq) is defined as one third of the trace of the orthogonalized Uij tensor

	x	*y*	*z*	U(eq)
C(3′a)	6531(1)	354(4)	6570(1)	43(1)
C(4′)	7153(1)	–931(5)	6810(1)	58(1)
C(5′)	7471(1)	–2851(5)	6411(1)	63(1)
C(6′)	7188(1)	–3553(5)	5790(1)	61(1)
C(7′)	6580(1)	–2319(5)	5542(1)	53(1)
C(7′a)	6275(1)	–362(4)	5940(1)	42(1)
O(1′)	5678(1)	1164(3)	5783(1)	47(1)
C(2′)	5564(1)	2827(4)	6329(1)	41(1)
C(3′)	6054(1)	2396(4)	6808(1)	44(1)
C(2)	4966(1)	4723(4)	6274(1)	39(1)
N(3)	4629(1)	5201(4)	5703(1)	51(1)
C(4)	4113(1)	7395(5)	5836(1)	60(1)
C(5)	4144(1)	7760(5)	6592(1)	52(1)
N(1)	4740(1)	6039(4)	6803(1)	56(1)

Powder diffraction

Two X-ray patterns were performed: a first one on the product after elaboration corresponding to the stable phase α, and the second one on a product after melting at 148°C of the stable phase which was then cooled down to room temperature with a cooling rate β= –50°C min, the X-ray analysis being performed immediately. In order to check whether the sample was going through decomposition totally or partially, DSC was performed. The temperature and the enthalpy of fusion measured were those of the metastable phase.

The results of the X-ray patterns are presented in Tables 7a and 7b.

Table 4 Bond lengths (Å) and angles (deg) for 1

C(3′a)-C(7′a)	1.388(3)
C(3′a)-C(4′)	1.401(3)
C(3′a)-C(3′)	1.424(3)
C(4′)-C(5′)	1.371(3)
C(5′)-C(6′)	1.389(3)
C(6′)-C(7′)	1.374(3)
C(7′)-C(7′a)	1.373(3)
C(7′a)-O(1′)	1.375(2)
O(1′)-C(2′)	1.381(2)
C(2′)-C(3′)	1.333(2)
C(2′)-C(2)	1.455(3)
C(2)-N(1)	1.312(2)
C(2)-N(3)	1.320(2)
N(3)-C(4)	1.469(3)
C(4)-C(5)	1.524(3)
C(5)-N(1)	1.454(2)
C(7a′)-C(3′a)-C(4′)	118.3(2)
C(7′a)-C(3′a)-C(3′)	105.6(2)
C(4′)-C(3′a)-C(3′)	136.1(2)
C(5′)-C(4′)-C(3′a)	118.1(2)
C(4′)-C(5′)-C(6′)	121.9(2)
C(7′)-C(6′)-C(5′)	121.2(2)
C(7′a)-C(7′)-C(6′)	116.4(2)
C(7′)-C(7′a)-O(1′)	125.9(2)
C(7′)-C(7′a)-C(3′a)	124.2(2)
O(1′)-C(7′a)-C(3′a)	110.0(2)
C(7′a)-O(1′)-C(2′)	105.7(1)
C(3′)-C(2′)-O(1′)	111.4(2)
C(3′)-C(2′)-C(2)	132.4(2)
O(1′)-C(2′)-C(2)	116.2(2)
C(2′)-C(3′)-C(3′a)	107.4(2)
N(1)-C(2)-N(3)	117.1(2)
N(1)-C(2)-C(2′)	120.4(2)
N(3)-C(2)-C(2′)	122.5(2)
C(2)-N(3)-C(4)	106.3(2)
N(3)-C(4)-C(5)	104.3(2)
N(1)-C(5)-C(4)	103.9(2)
C(2)-N(1)-C(5)	107.6(2)

Table 5 Anisotropic displacement parameters ($Å^2 \cdot 10^3$) for 1. The anisotropic displacement factor exponent takes the form: $-2\pi^2[h^2a^2U11+\ldots+2hkab\ U12]$

	U11	U22	U33	U23	U13	U12
C(3′a)	44(1)	46(1)	38(1)	4(1)	1(1)	4(1)
C(4′)	51(1)	68(2)	54(1)	3(1)	–10(1)	11(1)
C(5′)	48(1)	74(2)	68(1)	13(1)	4(1)	20(1)
C(6′)	63(1)	63(2)	57(1)	5(1)	19(1)	20(1)
C(7′)	61(1)	59(1)	40(1)	–4(1)	6(1)	11(1)
C(7′a)	40(1)	48(1)	39(1)	6(1)	3(1)	6(1)
O(1′)	48(1)	56(1)	36(1)	–2(1)	–3(1)	13(1)
C(2′)	45(1)	43(1)	33(1)	–1(1)	5(1)	4(1)
C(3′)	49(1)	49(1)	35(1)	–1(1)	–1(1)	8(1)
C(2)	40(1)	44(1)	33(1)	2(1)	2(1)	3(1)
N(3)	56(1)	64(1)	35(1)	–7(1)	–7(1)	20(1)
C(4)	60(1)	69(2)	52(1)	–9(1)	–13(1)	25(1)
C(5)	48(1)	60(1)	48(1)	0(1)	5(1)	13(1)
N(1)	60(1)	76(1)	31(1)	–4(1)	–1(1)	27(1)

Table 6 Hydrogen co-ordinates ($\cdot 10^4$) and isotropic displacement parameters ($Å^2 \cdot 10^3$) for 1

	x	*y*	*z*	U(eq)
H(4')	7345(1)	–494(5)	7227(1)	69
H(5')	7887(1)	–3707(5)	6562(1)	76
H(6')	7415(1)	–4883(5)	5536(1)	73
H(7')	6385(1)	–2784(5)	5128(1)	64
H(3')	6079(1)	3269(4)	7220(1)	53
H(3)	4698(1)	4390(4)	5328(1)	62
H(4A)	3636(1)	6876(5)	5689(1)	72
H(4B)	4250(1)	9067(5)	5610(1)	72
H(5A)	4231(1)	9655(5)	6710(1)	62
H(5B)	3701(1)	7166(5)	6795(1)	62
H(1)	4913(1)	5907(4)	7202(1)	67

Table 7a X-ray of the α-phase d/*I* file

Theta/degree	*d*-spacing/Å	I/I_0
4.605	9.594	29
4.725	9.351	100
6.335	6.981	19
6.450	6.857	23
7.965	5.559	9
8.810	5.029	83
9.355	4.738	10
9.995	4.438	11
10.375	4.277	39
11.490	3.867	33
11.710	3.795	62
12.280	3.621	16
12.865	3.459	11
13.240	3.363	42
14.280	3.123	25
14.500	3.076	22
14.950	2.986	35
15.120	2.953	12
15.625	2.860	7
16.000	2.794	7
16.480	2.715	11
16.975	2.638	7
17.445	2.569	7
17.865	2.511	15
19.265	2.334	7
19.695	2.285	10
20.175	2.233	8
21.435	2.108	6
21.965	2.059	5

In an approximation r is the radius of a germ which is assumed to be a sphere, G_v^s and G_v^1 are respectively the free energies of the solid and the liquid phases per unit volume, γ is the interfacial free energy.

Table 7b X-ray of the γ-phase d/*I* file

Theta/degree	*d*-spacing/Å	I/I_0
4.05	10.906	71
6.95	6.366	84
7.78	5.690	4
8.24	5.374	10
8.59	5.157	40
9.12	4.860	66
9.54	4.647	6
10.23	4.337	10
11.09	4.004	22
12.49	3.562	18
12.79	3.479	100
13.27	3.356	27
13.52	3.295	38
14.13	3.155	13
14.93	2.990	6
15.38	2.904	10
15.96	2.801	9
16.32	2.741	5
17.45	2.569	8
17.73	2.529	6
19.94	2.259	6
20.55	2.194	12
21.22	2.128	3

Discussion

It is well-known that thermodynamic equilibrium is reached with a low heating or cooling rate.

This is understandable if we consider the Gibbs energy function, $G=f(T)p$ of each phase, because, since there is a relation between T (temperature) and t (time), it is equivalent to have $G=f(t)p$.

In the case of monotropic behaviour for constant pressure we have the following scheme illustrated in Fig. 7: A is the stable melting point of α, B is the metastable melting point of γ. When the liquid is cooled, if the scanning rate is high no crystallisation is possible and the supercooled liquid (for $T<T_{fus\ \gamma}$) may reach point E. In this case E corresponds to a glass transition (T_g) and glass is induced.

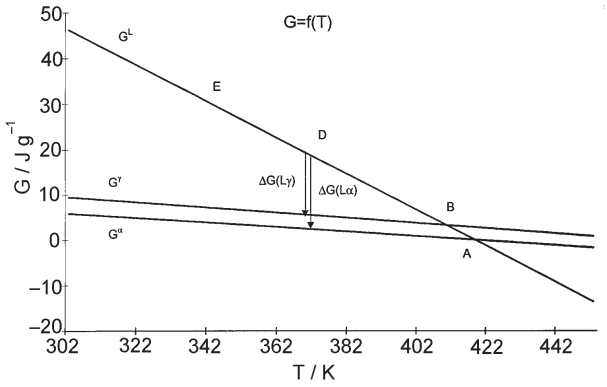

Fig. 7 $\Delta G = f(T)$ for α, γ and the liquid phase

If the liquid is cooled down to D, γ is more stable than the liquid and the 'driving energy' ΔG necessary to reach α is greater than that which is needed to reach γ. This difference increases as T decreases. In fact, the difference between these driving energies is inversely proportional to the cooling rate. From our measurements, we deduced that the difference between G^l and G^s (stable phase) is 28 J g^{-1} at 65°C and 15 J g^{-1} at 102°C, and the difference between the two G^s curves is of about 3 J g^{-1}.

One may assume in a first approximation that this driving energy is almost constant. In this case it is observed that it is easier to crystallise α when the minimum necessary difference is low.

If two reactions are possible, it means that there is a competition between the two reactions:

$$L \rightarrow \alpha \text{ and } L \rightarrow \gamma.$$

The easier reaction is the one which has the lowest free energy of activation. For these reactions of germination from a liquid, the free energy of activation is deduced from the theory of germination of Volner [8], the free energy of formation is the sum of two terms:

$$\Delta_f G = (4\pi r^3/3)(G_v^s - G_v^l) + 4\pi r^2 \gamma \tag{3}$$

This function first increases and then decreases; the maximum is reached when the derivative of the G function equals zero:

$$d\Delta_f G/dr = 4\pi r^2 (G_v^s - G_v^l) + 8\pi r\gamma \tag{4}$$

$$d\Delta_f G/dr = 0$$

From this equation the critical radius is deduced:

$$r^* = -(2\gamma)/(G_v^s - G_v^l) \tag{5}$$

When, during cooling, the temperature moves away from the melting temperature, G^s–G^l increases, and the radius decreases. When the radius is equal to the critical value, the free energy of formation of a solid germ corresponds to the free energy of activation and its value is:

$$\Delta G^* = (16\pi\gamma^3)/[3(G_v^s - G_v^1)^2] \quad (6)$$

If the molar volume of the liquid and of the solid are unknown, it is necessary to approximate the formula and to consider that molar volumes are equal for all the phases.

$$\Delta G^* = (16\pi\gamma^3 V^2)/[3(G^s - G^1)^2] \quad (7)$$

Using Eq. (2) for (G^s–G^l), we observe that the difference between the free energy of activation tends toward zero when (G^s–G^l) increases or when the difference between the temperature of fusion and the temperature of crystallisation increases during a cooling process. Thus it is possible to infer that an inversion occurs, for a temperature of crystallisation lower than 86°C; as a matter of fact because each volume has its proper law of variation *vs.* of the temperature ($V=f(T)$). The metastable phase γ should undergo a transformation reaction into α, in that case a calculation shows that the free energy of activation of this reaction is approximately fifty times as important as the one for the reactions of crystallisation from a liquid.

Conclusions

In the case of the study of the 2-(2-benzofuryl) Δ-2 imidazoline, the kinetic conditions are essential as regards obtaining the α stable phase. Only slow cooling rates must be used to obtain the α-phase from the liquid. Actually one must consider that the *G* function depends on time, and some components and systems are very sensitive to the cooling rate. Consequently the equilibrium state is usually difficult to reach.

References

1 C. B. Chapleo, P. L. Myers, R. C. M. Butler, J. A. Davis, C. J. Coxey, S. D. Higgins, M. Myers, A. G. Roach, C. F. Smith, M. R. Stillings and A. P. Welbourn, J. Med. Chem., 27 (1984) 570.
2 M. Anastassiadou, S. Danoun, L. Crane, G. Baziard-Mouysset, M. Payard, D. H. Caignard, P. Renard and M. C. Rettori, Bioorganic and Medicinal Chem., 9 (2001) 585.
3 J. K. Haleblian, R. T. Koda and J. A. Biles, J. Pharm. Sci., 60 (1971) 1488.
4 Note of the Editor, Bull. Alloy Phases Diagrams, 7 (1986) 602.
5 Hultgren et al., 1973. 'Selected Values of the Thermodynamic Properties of the elements', A. S. M. Materials Park 1973.
6 B. Fraisse, 1985. Thèse Univ. Montpellier II.
7 G. M. Sheldrick,1993. SHELXS93. Program for refinement of crystal structures. Univ. of Göttingen, Germany.
8 M. Volner and A. Weber, Z. Phys. Chem., 119 (1925) 277.